doi.org/10.36721/PJPS.2026.39.1.REG.14756.1

Syringaresinol inhibits ferroptosis and ameliorates glucocorticoid-induced MC3T3-E1 osteoporosis by modulating the Nrf2/SLC7A11/GPX4 pathway

Shaojing Wang[1] and Guoying Zhang[2]*

[1]Department of Pharmacy, Affiliated Hospital of Shandong University of Traditional Chinese Medicine, Jinan, Shandong province, China

[2]Department of Trauma and Hand and Foot Surgery, Shandong Provincial Third Hospital, Shandong University, Jinan, China

Abstract: **Background**: Osteoporosis (OP) is closely related to osteoblast damage and abnormal activation of ferroptosis. **Aims**: To investigate whether natural polyphenolic compound syringaresinol (Syr) improves OP by activating the Nrf2/solute carrier family 7 member 11 (SLC7A11)/glutathione peroxidase 4 (GPX4) pathway. **Methods**: A dexamethasone (DEX)-induced osteoblast injury model of MC3T3-E1 was established and the impacts of Syr on cell viability were assessed using Cell Counting Kit-8 and lactate dehydrogenase (LDH) assay. Osteogenic differentiation of MC3T3-E1 cells was assessed by alkaline phosphatase (ALP) staining, Alizarin Red S (ARS) staining and different kits. Oxidative stress factors and Fe^{2+} content were examined by flow cytometry and different kits. The levels of bone formation, ferroptosis and Nrf2/SLC7A11/GPX4 pathway-related proteins were examined through western blot. **Results**: Syr at concentrations of 25, 50, and 100 μM did not negatively impact MC3T3-E1 cell viability, and was able to enhance the viability of DEX-treated MC3T3-E1 cells and inhibit LDH release. Syr effectively increased ALP activity and ARS stained area and up-regulated bone formation marker proteins in MC3T3-E1 cells. Additionally, Syr inhibited oxidative stress and decreased ferroptosis-related protein levels. Notably, Syr activated Nrf2/SLC7A11/GPX4 pathway. Silencing Nrf2 impaired the ameliorative impact of Syr on osteogenic function and caused oxidative stress and ferroptosis. **Conclusion**: Syr inhibits ferroptosis, promotes osteogenesis in MC3T3-E1 cells and ameliorates DEX-induced OP by activating Nrf2/SLC7A11/GPX4 pathway.

Keywords: Dexamethasone; Ferroptosis; Nrf2/SLC7A11/GPX4 pathway; Osteoporosis; Syringaresinol

Submitted on 21-06-2025 – Revised on 13-08-2025 – Accepted on 15-09-2025

INTRODUCTION

As the population grows older, osteoporosis (OP) is emerging as a critical public health concern, with rising rates of incidence (Johnston and Dagar, 2020; Yong and Logan, 2021). In China, approximately 20.73% of middle-aged and older men are affected, whereas the rate for women in the same age group reaches an impressive 38.05%, which is due to the imbalance between bone formation and bone degradation caused by the decrease in estrogen level after menopause (Fischer and Haffner-Luntzer, 2022; Walker and Shane, 2023; Wang *et al.*, 2023a). There is a dynamic equilibrium of bone reconstruction processes in bone tissue and an imbalance in bone reconstruction is the core pathogenesis of OP, with increased osteoclast activity and suppressed osteoblast function leading to sustained bone loss, which in turn leads to fragile bones and an increased risk of fracture (Kim *et al.*, 2020; Wu *et al.*, 2024b; Zhong *et al.*, 2025). Among its various etiologies, glucocorticoid-induced OP (GIOP) stands out as a major form of secondary OP, affecting approximately 30-50% of patients receiving long-term glucocorticoid therapy (e.g., dexamethasone, DEX) (Jha, 2023; Madrid *et al.*, 2025). Glucocorticoids disrupt bone metabolism by suppressing osteoblast proliferation and differentiation, promoting osteoblast apoptosis and exacerbating osteoclast activity, with recent evidence highlighting ferroptosis as a critical driver of glucocorticoid-induced osteoblast dysfunction (Urquiaga and Saag, 2022; Ochiai *et al.*, 2024). Current treatments for OP include calcium supplementation, inhibition of osteoclast activity, promotion of osteoblast proliferation and estrogen replacement therapy, but drugs that promote bone formation are limited and have potential side effects (Muñoz *et al.*, 2020; Brown, 2021; Zhang *et al.*, 2024). Therefore, it is extremely necessary to explore new strategies to regulate osteoblast function and improve OP.

Chinese medicines and their extracts are not only safe but also have rich pharmacological activities and multi-targeting properties, which have attracted much attention in the therapeutic studies of OP and osteoarthritis (Wang *et al.*, 2020; Wang *et al.*, 2024c; Qiao *et al.*, 2025). It has been shown that phytoestrogens with a polyphenolic structure can bind to estrogen receptors in the human body, mimicking the effects of estrogen and having the therapeutic potential to replace estrogen (Jang *et al.*, 2022). Syringaresinol (Syr) is a natural lignan that is mainly present in *Eucommia ulmoides* and *Sargentodoxae and* is also a phytoestrogen with a polyphenolic structure. It can

**Corresponding author:* e-mail: zgy21769e_@hotmail.com

also be extracted from oilseeds, grain husks and various berry seeds (Jang *et al.*, 2022; Zhang *et al.*, 2025). Syr exhibits multiple pharmacological effects, like anti-inflammatory, antioxidant and immunomodulatory impacts and has shown potential application in osteoarthritis, cardiorenal fibrosis and diabetic nephropathy treatment (Li *et al.*, 2023a; Wang *et al.*, 2023b; Wang *et al.*, 2023c). Syr showed a linear pharmacokinetic profile in rats after oral administration, exhibiting slow absorption and wide distribution (Zhang *et al.*, 2025). In addition, Syr has a high safety profile, with studies showing that 100 μM Syr does not cause HepG2 and HT29 cytotoxicity (Kirsch *et al.*, 2020). Syr has been shown to inhibit the secretion of inflammatory factors, thereby reducing osteoarthritis (Wang *et al.*, 2023c). Also, a natural polyphenol curcumin has been reported to alleviate GIOP by modulating the gut microbiota (Li *et al.*, 2025). However, at present, the studies on the pharmacological activity of Syr are still not deep enough and the effect of Syr on OP, along with its underlying mechanisms, has yet to be clarified.

Ferroptosis, distinct from apoptosis, necrosis, or pyroptosis, is an iron-dependent form of regulated cell death characterized by imbalances in iron regulation, weakened defenses against oxidative stress and excessive lipid peroxidation (Jiang *et al.*, 2021; Ashrafizadeh, 2024; Dixon and Olzmann, 2024). Ferroptosis and metabolic disorders are closely linked and OP, as a representative of abnormal bone metabolism, is intricately related to each other (Wang *et al.*, 2025). Interfering with bone metabolic status by modulating cellular ferroptosis in order to influence OP development has become one of the important research directions in this field (Wang *et al.*, 2024b; Wu *et al.*, 2024a). The nuclear factor E2-related factor 2 (Nrf2) is a master regulator of cellular redox homeostasis and a critical suppressor of ferroptosis, plays a crucial role in managing the cellular response to oxidative stress, it is normally inactivated by binding to the repressor protein Keap1 (Morgenstern *et al.*, 2024; Wang *et al.*, 2024a).

In response to oxidative stress or iron overload, Nrf2 detaches from Keap1 and moves into the nucleus, upregulates antioxidant genes, including solute carrier family 7 member 11 (SLC7A11) and glutathione peroxidase 4 (GPX4) (Yuan *et al.*, 2021; Liu *et al.*, 2023). Nrf2, GPX4 and SLC7A11 have been shown to have significant antioxidant functions to block and reverse ferroptosis in osteoblasts (Zhang *et al.*, 2022b; Deng *et al.*, 2024). However, whether Syr can alleviate OP by modulating the Nrf2/SLC7A11/GPX4 pathway remains unexamined. Therefore, this study established a dexamethasone (DEX)-induced MC3T3-E1 cell injury model with the aim of investigating whether Syr exerts an anti-OP effect by regulating this pathway and providing experimental basis and theoretical support for Syr clinical application and OP therapeutic drugs development.

MATERIALS AND METHODS

Cell culture and treatment

Mouse embryonic osteoblast precursor cells MC3T3-E1 (SNL-021) were purchased from Sunncell Biotechnology (Wuhan, Hubei, China). Cells were placed in sterile culture flasks and cultured using complete medium containing 10 % fetal bovine serum (SNS-001, Sunncell Biotechnology), 1% penicillin/streptomycin (SNA-001, Sunncell Biotechnology) and 89% DMEM (SNM-002B, Sunncell Biotechnology) in complete medium for culture. Subsequently, the culture medium was supplemented with 40 ng/mL DEX (ST1258, Beyotime, Shanghai, China), 50 μg/mL ascorbic acid (HY-B0166, MedChemExpress, Monmouth Junction, NJ, USA) and 10 mM β-glycerophosphate (G5422, Sigma-Aldrich, St. Louis, MO, USA), when the cells achieved 70% confluence, which was considered to be the completion of osteogenic induction (Zhu *et al.*, 2022). Referring to Han *et al*, MC3T3-E1 cells were exposed to DEX (1 μM) for 24 h to mimic the OP model (Han *et al.*, 2019).

In an experiment to investigate the effect of Syr (HY-126030, MedChemExpress) on cell viability, MC3T3-E1 cells were exposed to Syr (12, 25, 50, 100, 200, or 300 μM) for 24 h (Wang *et al.*, 2023c). When exploring the inhibitory impact of Syr on OP, MC3T3-E1 cells were first exposed to DEX for 24 h to induce OP, followed by treatment with varying doses of Syr for 24 h.

Nrf2 small interfering RNA (si-Nrf2) and control (si-NC) were synthesized by RiboBio Co., Ltd. (Guangzhou, Guangdong, China). Following the guidelines for Lipofectamine 3000 (L3000001, Invitrogen, Carlsbad, CA, USA), si-Nrf2 and si-NC were introduced into MC3T3-E1 cells. After 48 h of transfection, MC3T3-E1 cells were exposed to DEX for 24 h and then to Syr (100 μM) for 24 h (Yao *et al.*, 2023). They were recorded as DEX+Syr100+si-NC group and DEX+Syr100+si-Nrf2 group, respectively. All experiments were limited to cell culture and performed according to standard lab protocols.

Cell Counting Kit-8 (CCK-8) assay

MC3T3-E1 cells were taken, digested by trypsin (HY-K3009, MedChemExpress) and resuspended in complete medium. Cells were seeded into 96-well plates (2.5×10^3 cells/100 μL) and, when the cells were fully apposed, exposed to DEX or/and Syr for 24 h. After that, added 10% CCK-8 reagent (HY-K0301, MedChemExpress) and left to incubate at 37°C for 2 h. To screen for appropriate concentrations for Syr treatment, OD_{450} values were examined through a microplate reader (SpectraMax iD3, Molecular Devices, Shanghai, China).

Lactate dehydrogenase (LDH) assay

LDH is a cytoplasmic enzyme that is unable to pass through normal cell membranes, so cell membrane

integrity can be assessed by measuring the amount of LDH released (Pandarathodiyil *et al.*, 2022). MC3T3-E1 cells were seeded into 96-well plates and once they reached approximately 70% confluence, they were exposed to DEX or/and Syr for 24 h. The supernatant was collected by centrifugation, mixed well with the LDH assay working solution (C0016, Beyotime) and incubated for 30 min at 25°C. The OD_{490} value of the cells was examined through a microplate reader to calculate the relative LDH release.

Reverse transcription quantitative polymerase chain reaction (RT-qPCR) assay

RNA in cells was extracted with Trizol (10606ES60, Yeasen, Shanghai, China), reverse transcribed (2621, TAKARA, Tokyo, Japan) to cDNA. The target genes were then amplified using the TB Green FAST qPCR kit (CN830S, TAKARA). GAPDH was utilized as the internal standard and the $2^{-\Delta\Delta Ct}$ method was applied to determine the relative gene expression level.

The primers used were as follows: mouse transferrin receptor 1 (TFRC)-F: 5'-GTTTCTGCCAGCCCCTTATTAT-3'; mouse TFRC-R: 5'-GCAAGGAAAGGATATGCAGCA-3'; mouse acyl-CoA synthetase long-chain family member 4 (ACSL4)-F: 5'-TGAACGTATCCCTGGACTAGG-3'; mouse ACSL4-R: 5'-TCAGACAGTGTAAGGGGTGAA-3'; mouse ferroptosis suppressor protein 1 (FSP1)-F: 5'-CGGGTTCGCCAAAAAGACATT-3'; mouse FSP1-R: 5'-CTATGCCAATCACTTTGCCCT-3'; mouse GAPDH-F: 5'-AGGTCGGTGTGAACGGATTTG-3'; mouse GAPDH-R: 5'-GGGGTCGTTGATGGCAACA-3'.

Alkaline phosphatase (ALP) assay

ALP staining: MC3T3-E1 cells were seeded into 6-well culture plates (2×10^4 cells/well) and cultured in DMEM medium (including DEX or/and Syr) for 2 d. After that, they were replaced with osteogenic differentiation medium (including DEX or/and Syr) to continue the culture. After 7 d of culture, cells were fixed using 4% paraformaldehyde (441244, Sigma-Aldrich) for half an hour (Yao *et al.*, 2023). Subsequently, the BCIP/NBT ALP reagent (C3206, Beyotime) was used for light-avoidance staining and the staining duration was 30 min. The color development reaction could be terminated by gently rinsing with distilled water for 2 times, followed by photographic observation using a microscope (DM IL LED, Leica, Heidelberg, Germany). The stained area of the experimental and control groups was analyzed by Image J software (1.54h, Wavne Resband, National Institute of Mental Health, USA) to quantify the relative activity of ALP.

ALP activity: In addition, ALP activity was examined through an ALP assay kit (P0321S, Beyotime) (Zhao *et al.*, 2020). After 7 days of culture as described above, MC3T3-E1 cells were lysed by cell lysis solution (P0013J, Beyotime) and centrifuged in the centrifuge (JRA-2800L, Wuxi Jie Ruian Instrument Equipment Co., Ltd, Jiangsu, China) for supernatants. The assay buffer, color development substrate and cell supernatant were mixed well and left to incubate at 37°C for 10 min. Subsequently, the reaction was terminated by the reaction termination solution. Finally, the OD_{405} values were examined through a microplate reader to calculate the ALP activity. Standardized according to the kit instructions using control group ALP activity as a reference.

Alizarin Red S (ARS) staining

MC3T3-E1 cells were cultured in DMEM medium (including DEX or/and Syr) for 2 d and then they were replaced with osteogenic differentiation medium (including DEX or/and Syr) to continue the culture. After 21 d of incubation, fixation was carried out using 4% paraformaldehyde for half an hour and PBS was gently rinsed three times to make sure that the fixative had been completely removed (Zou *et al.*, 2024). Subsequently, added ARS staining solution (C0148S, Beyotime) for staining for 30 min and rinsed twice with PBS, then observed using a microscope. To assess MC3T3-E1 cell mineralization capacity, images were processed by ImageJ software to quantify the relative activity of ARS.

Enzyme-Linked immunosorbent assay (ELISA)

Mouse runt-related transcription factor 2 (Runx2, ml603125S), Osteopontin (OPN, ml001898), osteocalcin (OCN, ml063317) ELISA kits were from Enzyme Link Biotechnology (Shanghai, China). Mouse bone morphogenetic protein 2 (BMP2, HJ270) ELISA Kit from Epizyme Biotech (Shanghai, China). After different treatments, MC3T3-E1 cells were centrifuged and supernatants were collected. 50 μL of cell supernatant, 50 μL of diluted standard and 50 μL of biotin-labeled antibody were introduced into the ELISA well plate, then incubated at 37°C for 60 min in the incubator (LRH-70F, Wuxi Marit Technology Co., Ltd, Jiangsu, China). The liquid in the wells was discarded, washed with washing solution, added HRP-labeled Streptavidin and left to incubated for 30 min away from light. Then added substrate A and substrate B, gently shook and mixed well and incubated at 37℃ away from light for 10 min. The termination solution was quickly introduced and well-mixed and then OD_{450} value was measured.

Flow cytometry

After different treatments, MC3T3-E1 cells were rinsed two times with PBS, centrifuged, the supernatant was discarded. The 2′,7′-dichlorofluorescein diacetate (DCFH-DA) fluorescent probe (HY-D0940, MedChemExpress) was mixed with the cells and serum-free culture medium to give a final concentration of 10 μM of DCFH-DA and incubated for 20 min in the dark. Upside down mixing was done every 3 to 5 min. The cell sediment was collected after centrifugation and rinsed with PBS for two times. Finally, the precipitate was resuspended with an appropriate amount of serum-free medium and transferred

to a flow-through tube. Detection was performed through BD FACSCalibur™ flow cytometer (BD Biosciences, San Jose, CA, USA) and reactive oxygen species (ROS) levels were calculated using FlowJo software (v10.8, BD Biosciences).

Superoxide dismutase (SOD), glutathione (GSH) and malondialdehyde (MDA) assay

MC3T3-E1 cells were washed once with pre-cooled PBS after different treatments. Cells were mixed well with SOD sample preparation solution (S0101S, Beyotime), lysed the cells well and centrifuged and took the supernatant as the sample to be tested. Protein content was examined through BCA Protein Assay Kit (ab102536, Abcam, Cambridge, MA, USA). A total of 50 μg of protein was mixed well with SOD assay buffer, incubated for half an hour at 37°C and the absorbance was recorded at 450 nm using Spectra Max iD3 microplate reader (Zheng *et al.*, 2025). Additionally, the supernatant from the previously mentioned cell lysate was taken and MDA and GSH levels were detected in accordance with the guidelines provided by MDA Assay kit (S0131S, Beyotime) and GSH Assay kit (BC1175, Solarbio, Beijing, China).

Fe^{2+} level assay

Ferro Orange Fluorescent staining: MC3T3-E1 cells were seeded in 6-well cell culture plates with pre-prepared sterile coverslips at a suitable density and when the cells grew until the fusion reached 70%-80%, the coverslips were carefully removed and gently rinsed twice with serum-free medium. Subsequently, 1 μM Ferro Orange Fluorescent Probe (HY-D1913, MedChemExpress) was added drop wise to the cell surface to ensure that the probe evenly covered the cells and incubated for half an hour under light protection. At the end of incubation, without washing, the cells were immediately placed under a microscope for observation and the fluorescence images of the cells were processed by ImageJ software to obtain fluorescence intensity.

Fe^{2+} content assay: Fe^{2+} levels were examined through the Fe^{2+} assay kit (ab83366, Abcam). Log phase MC3T3-E1 cells were taken and resuspended in PBS. Under ice bath conditions, the homogenization process was carried out by adding 5 times the volume of the iron assay buffer and the homogenized supernatant was gathered. Subsequently, iron reducing agent was mixed well with the supernatant, incubated for 30 min in the dark, then added iron probe, mixed well again and incubated for 60 min. After the incubation was completed, the OD_{593} value was quickly examined through microplate reader and a standard curve was plotted to calculate the intracellular Fe^{2+} content.

Western blot

After MC3T3-E1 cells were treated differently, the cell precipitate was collected by centrifugation, RIPA lysis buffer (P0013B, Beyotime) was added and mixed and the cells were lysed sufficiently to extract proteins. After lysis was completed, the protein levels in the samples were assessed by the BCA protein assay kit. Next, the protein was mixed well with SDS-PAGE protein upsampling buffer, followed by the separation of proteins through SDS-PAGE electrophoresis. Subsequently, proteins were transferred to PVDF membranes (Invitrogen) and closed with 5% bovine serum albumin (BSA, B2064, Sigma-Aldrich) for 2 h. After that, the membranes were incubated overnight with primary antibodies Bmp2 (PA5-85956, 1:1000, Invitrogen), Runx2 (PA5-82787, 1:2000, Invitrogen), ACSL4 (MA5-42523, 1:1000, Invitrogen), OPN (PA5-34579, 1:500, Invitrogen), OCN (PA5-96529, 1:500, Invitrogen), TFRC (ab214039, 1:1000, Abcam), FSP1 (ab155326, 1:500, Abcam), SLC7A11 (MA5-35360, 1:500, Invitrogen), GPX4 (MA5-32827, 1:10000, Invitrogen), or Nrf2 (PA5-27882, 1:3000, Invitrogen) at 4°C. The following day, after washing the membrane 3 times, the secondary antibody (ab205718, 1:10000, Abcam) was incubated for 2 h. Developing solution (HY-K2005, MedChemExpress) was prepared, dropped evenly on the membrane and scanned with 5200 Multi gel imaging system (Tanon, Shanghai, China). GAPDH (MA5-35235, 1:50,000, Invitrogen) was used as an internal reference protein and the relative protein expression levels were quantified by analyzing the ratio of gray scale values of the target proteins to those of the internal reference proteins by ImageJ software. In addition, the Nuclear and Cytoplasmic Protein Extraction Kit (P0028, Beyotime) was utilized to extract nuclear proteins from MC3T3-E1 cells. Nrf2 level in the nucleus was determined according to the above method using Lamin B1 (702972, 1:3000, Invitrogen) as an internal reference.

Statistical analysis

All experiments were performed with 3 biological replicates per group and each biological replicate was analyzed with 3 technical replicates. Results are presented as mean ± standard deviation. Statistical analyses were conducted using SPSS 26.0 software (IBM SPSS Statistics 26) and graphs were generated using GraphPad Prism 9.0 software. For statistical testing, normality of the data was first assessed using the Shapiro-Wilk test and homogeneity of variance was evaluated using Levene's test. For multiple group comparisons, one-way analysis of variance (ANOVA) was applied. When variances were homogeneous, pairwise comparisons were performed using the LSD test; when variances were heterogeneous, Tamhane's T2 test was used for pairwise comparisons. $P<0.05$ represents a statistically significant difference.

RESULTS

Syr ameliorates DEX-induced reduction in MC3T3-E1 cell activity

Fig. 1A shows the molecular formula of Syr. The viability of normal MC3T3-E1 cells after 24 hours of exposure to various concentrations of Syr treatment was detected through the CCK-8 assay. Syr at 12, 25, 50 and 100 μM did

not notably impact cell survival (P>0.05), whereas increasing the dosage to 200, 300, 600 and 1200 μM caused a marked reduction in cell viability, which indicated that the high dose of Syr had some cytotoxicity (Fig. 1B). DEX (1 μM) treatment significantly decreased MC3T3-E1 cell viability to 66.11% (P<0.01), whereas Syr treatments of 25, 50, 100 and 200 μM increased the cell viability after DEX treatment (P<0.05) (Fig. 1C). The results of LDH assay showed that DEX caused an 88% marked rise in LDH release from MC3T3-E1 cells (P<0.001), whereas Syr treatment at 25, 50, 100, 200 and 300 μM significantly inhibited LDH release (P<0.05) (Fig. 1D). These results suggested that Syr can alleviate DEX-induced reduction in MC3T3-E1 cell activity and inhibit LDH release. Due to the cytotoxicity of 200 and 300 μM Syr, we chose 25, 50 and 100 μM Syr for subsequent experiments.

Syr ameliorates DEX-induced reduction of osteogenic function

Next, we investigated the impact of Syr treatment on the osteogenic function of MC3T3-E1 cells. ALP staining revealed that DEX treatment caused lighter staining of MC3T3-E1 cells and a 78% reduction in the number of ALP-positive cells compared to control group (P<0.001), whereas Syr treatment attenuated the effect of DEX (P<0.01) (Figs. 2A-2B). ALP quantification results similarly showed that after DEX treatment, ALP activity was significantly reduced by 27 U/L in MC3T3-E1 cells (P<0.001) and Syr treatment dose-dependently increased ALP activity, which was the same as the staining results (P<0.01) (Fig. 2C). In addition, by ARS staining, we found that DEX treatment reduced the ARS-positive area of MC3T3-E1 cells by 85% (P<0.001), indicating a decline in the number of mineralized nodules, while mineralized nodules numbers were increased markedly after Syr treatment (P<0.05) (Figs. 2D-2E). ELISA results revealed that bone formation markers like Runx2, Bmp2, OCN and OPN levels were significantly reduced in cell supernatant after DEX treatment (P<0.001), whereas Syr treatment weakened the treatment effect of DEX and increased Runx2, Bmp2, OCN and OPN levels (Figs. 2F-2I). Not only that, Western blot likewise showed that DEX caused a marked decline in Runx2, Bmp2, OCN and OPN expression (P<0.001) and Syr treatment weakened the effect of DEX (P<0.05) (Figs. 2J-2N). These findings confirmed that DEX reduced the differentiation activity and declined the osteogenic capacity of MC3T3-E1 cells, whereas Syr effectively increased the differentiation activity and osteogenic capacity of the cells.

Syr ameliorates DEX-induced oxidative stress and ferroptosis

It has been shown that oxidative stress and ferroptosis play a key role in the pathology of OP (Liu *et al.*, 2022). Therefore, we explored whether Syr attenuates DEX-induced MC3T3-E1 cell injury and reduced osteogenic capacity through hindering oxidative stress and ferroptosis. Flow cytometry revealed that DEX treatment resulted in a significant 320% rise in ROS levels (P<0.001), whereas Syr was able to attenuate the impact of DEX, resulting in a significant decrease in ROS levels (P<0.05) (Figs 3A-3B). Furthermore, DEX notably elevated the lipid peroxidation marker MDA levels and notably declined SOD and GSH levels (P<0.001), whereas Syr treatment reversed the impact of DEX (P<0.05) (Figs. 3C-3E). By FerroOrange staining, we found that DEX treatment caused a marked rise in Fe^{2+} content (P<0.001) and the Fe^{2+} assay kit results also showed a significant increase in Fe^{2+} levels (P<0.001), whereas Syr treatment caused a significant decline in Fe^{2+} levels (P<0.05) (Figs. 3F-3H).

In addition, DEX treatment markedly elevated the levels of the ferroptosis marker TFRC (171% increase) and ACSL4 (234% increase) proteins and declined FSP1 (74% reduction) level in MC3T3-E1 cells (P<0.001), but Syr treatment notably reversed the effect of DEX (P<0.05) (Figs. 3I-3J). Not only that, DEX treatment increased TFRC (131% increase) and ACSL4 (221% increase) mRNA levels and decreased FSP1 (73% reduction) levels in MC3T3-E1 cells (P<0.001), whereas Syr treatment significantly reversed the effects of DEX (P<0.05) (Fig. 3K). These suggested that DEX promoted oxidative stress and ferroptosis, while Syr ameliorated DEX-induced cellular oxidative stress and ferroptosis.

Syr modulates the Nrf2/SLC7A11/GPX4 signaling pathway

We investigated the molecular mechanisms through which Syr improves osteogenic function and ferroptosis in MC3T3-E1 cells by assessing the associated signaling pathways. DEX treatment significantly reduced SLC7A11, GPX4 and nuclear Nrf2 levels by 90%, 67% and 85% in MC3T3-E1 cells (P<0.001), whereas total Nrf2 protein levels were not significantly changed (P>0.05). Syr treatment, on the other hand, increased SLC7A11, GPX4, nuclear Nrf2 and total Nrf2 proteins expression, suggesting that Syr activates the Nrf2/SLC7A11/GPX4 pathway (Figs. 4A-4E). After transfection of si-Nrf2, the protein level of Nrf2 was notably reduced by 38% in MC3T3-E1 cells (P<0.01), confirming that the transfection was successful and subsequent experiments could be performed (Figs. 4F-4G). Transfection of si-Nrf2 in MC3T3-E1 cells markedly attenuated the impact of Syr, resulting in a significant decline of SLC7A11, GPX4, total Nrf2 and nuclear Nrf2 levels by 16%, 14%, 75% and 20% in MC3T3-E1 cells (P<0.05) (Figs. 4H-4L). These results confirmed that DEX blocked Nrf2/SLC7A11/GPX4 pathway in MC3T3-E1 cells, whereas Syr activated this pathway.

Syr mediates the Nrf2/SLC7A11/GPX4 pathway to improve osteogenic function

Next, we explored whether Syr ameliorates DEX-induced decline in osteogenic function of MC3T3-E1 cells through activating the Nrf2/SLC7A11/GPX4 pathway. The intensity of ALP staining was significantly enhanced by 73% in Syr-treated MC3T3-E1 cells (P<0.001), indicating that

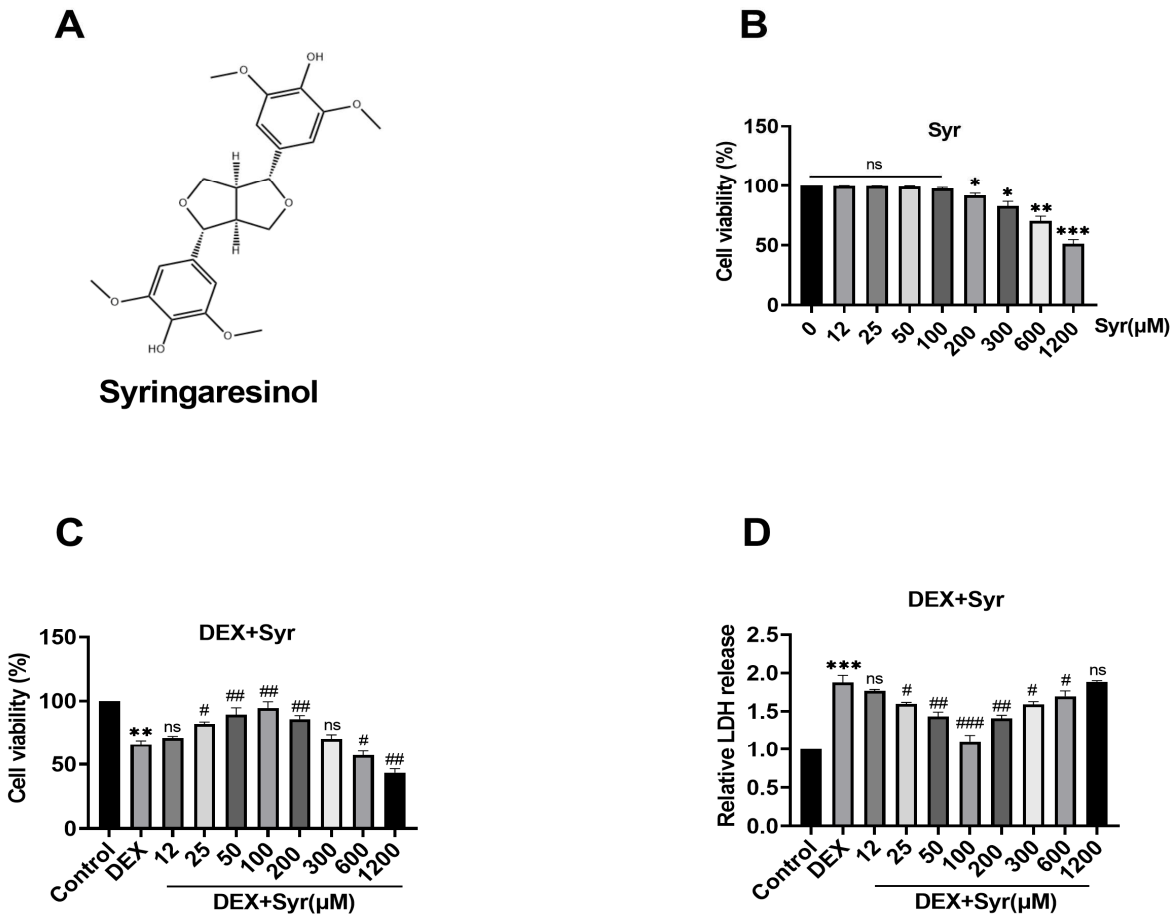

Fig. 1: Syr ameliorates DEX-induced reduction in MC3T3-E1 cell activity (A) The chemical structure formula of Syr. (B) CCK-8 assay detected the viability of MC3T3-E1 cells following a 24-hour exposure to various concentrations of Syr. (C) CCK-8 assay detected the viability of DEX-treated MC3T3-E1 cells following a 24-hour exposure to Syr. (D) LDH assay measured LDH release in DEX-treated MC3T3-E1 cells. n=3, **P*<0.05, ***P*<0.01, ****P*<0.001 vs Control, ns *P*≥0.05, #*P*<0.05, ##*P*<0.01, ###*P*<0.001 vs DEX.

Syr could effectively increase the differentiation activity of this cell and promote its differentiation towards osteoblasts. And when cells were transfected with si-Nrf2, the enhancement of differentiation activity brought about by Syr treatment was significantly attenuated (*P*<0.01) (Figs. 5A-5C). Syr treatment caused a notable 75% rise in the number and staining intensity of mineralized nodules in MC3T3-E1 cells (*P*<0.001), suggesting that Syr is effective in enhancing the mineralization capacity of these cells and promoting the formation of bone matrix.

The enhancement effect of mineralization capacity induced by Syr treatment was significantly inhibited by 49% after transfection with si-Nrf2 (*P*<0.01) (Figs. 5D-5E). In addition, Runx2, OPN and OCN levels in the cell supernatants of the Syr-treated group were markedly higher than the DEX-treated group (*P*<0.01), suggesting that Syr promoted the synthesis and secretion of these osteogenesis-related proteins. In contrast, after silencing Nrf2, the levels of all three proteins in the cell supernatant showed a significant decrease (*P*<0.05) (Figs. 5F-5I). Syr treatment caused a significant rise in Runx2, OPN and OCN protein levels in MC3T3-E1 cells (*P*<0.05), indicating that Syr not only promoted the secretion of these proteins but also increased their expression within the cells. And the levels of all three proteins were significantly reduced after transfection with si-Nrf2 (*P*<0.05) (Figs. 5J-5N). This confirms that Syr may improve the osteogenic function of MC3T3-E1 cells through activating the Nrf2/SLC7A11/GPX4 pathway.

Syr mediates the Nrf2/SLC7A11/GPX4 pathway to ameliorate DEX-induced oxidative stress and ferroptosis

Finally, we explored whether Syr alleviated DEX-induced oxidative stress and ferroptosis in MC3T3-E1 cells through activating Nrf2/SLC7A11/GPX4 pathway. ROS levels were notably reduced by 183% after Syr treatment, which indicated that Syr was able to effectively scavenge intracellular ROS (*P*<0.001). Whereas, when cells were transfected with si-Nrf2, ROS levels were significantly elevated by 62% (*P*<0.01) (Figs. 6A-6B). Syr treatment weakened the effect of DEX, resulting in a marked decline

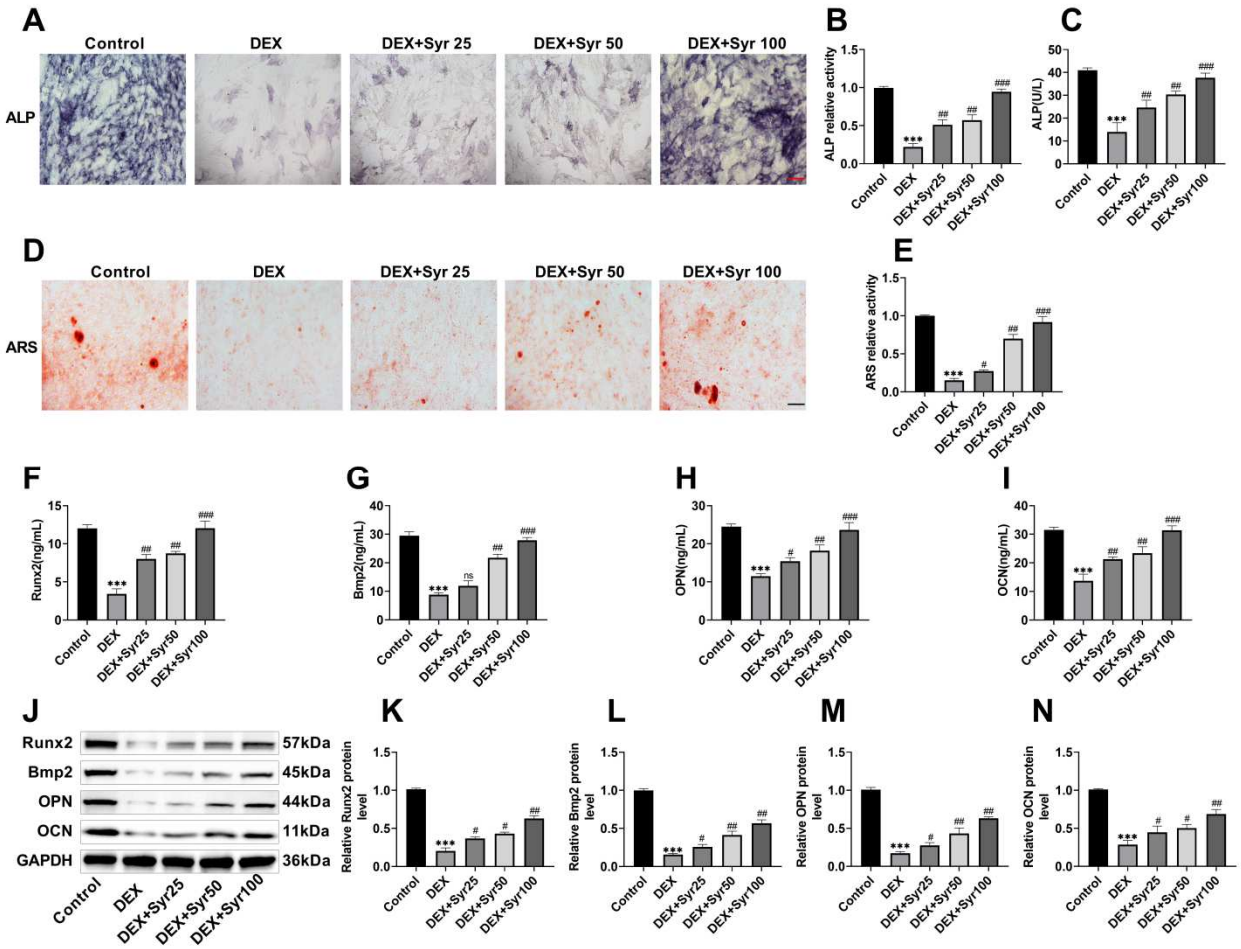

Fig. 2: Syr ameliorates DEX-induced reduction of osteogenic function (A-C) ALP staining showed measured DEX declined the ALP activity of MC3T3-E1 cells, which was reversed by Syr treatment (20×, 100 μm). (D-E) ARS staining showed that DEX decreased the mineralization capacity, whereas Syr treatment increased the mineralization capacity (20×, 100 μm). (F-I) The ELISA kit measured that DEX decreased Runx2, OPN and OCN levels in the cell supernatant, and Syr treatment increased these levels. (J-N) Western blot measured Runx2, OPN and OCN levels in MC3T3-E1 cells. n=3, ***P<0.001 vs Control, ns P≥0.05, #P<0.05, ##P<0.01, ###P<0.001 vs DEX.

in MDA level in MC3T3-E1 cells, along with a notable rise in SOD and GSH levels (P<0.001). However, when transfected with si-Nrf2, the effect of Syr was reversed and intracellular MDA levels rebounded and SOD and GSH levels decreased (P<0.01) (Figs. 6C-6E). After Syr treatment, the intensity of Fe^{2+} fluorescence in MC3T3-E1 cells was markedly weakened, while Fe^{2+} content assay also indicated that its level was significantly reduced (P<0.001). After silencing Nrf2, the intensity of intracellular Fe^{2+} fluorescence was significantly enhanced and Fe^{2+} levels were significantly elevated (P<0.01) (Figs. 6F-6H). Not only that, after Syr treatment, the protein levels of TFRC and ACSL4 decreased by 107% and 133% and the protein level of FSP1 increased by 69% (P<0.01). However, after silencing Nrf2, TFRC and ACSL4 expression levels rebounded by 105% and 102% and FSP1 levels decreased by 36% (P<0.05) (Figs. 6I-6J). Similar trends were observed for mRNA levels of Nrf2, TFRC and ACSL4 (Figs. 6K). These findings implied that Syr attenuated the oxidative stress and ferroptosis triggered by DEX through activating the Nrf2/SLC7A11/GPX4 pathway.

DISCUSSION

OP patients are at increased risk of fractures, raising disability and mortality rates among elderly patients (Clynes *et al.*, 2020; Lo *et al.*, 2023). The main drugs commonly utilized in the clinical management of OP are bisphosphonates, estrogens and calcium, but these drugs are associated with adverse effects, drug dependence and other problems (Sabri *et al.*, 2023). Therefore, it is urgent to explore novel drugs against OP. In recent years, natural plant extracts have become a research hotspot due to their unique biological activities. DEX is a clinically used glucocorticoid that can cause OP with prolonged use and is frequently employed to construct experimental OP cell injury models (Zhang *et al.*, 2022a). Referring to previous studies (Han *et al.*, 2019; Zheng *et al.*, 2021), we treated MC3T3-E1 cells with DEX (1 μM) to construct an OP cell

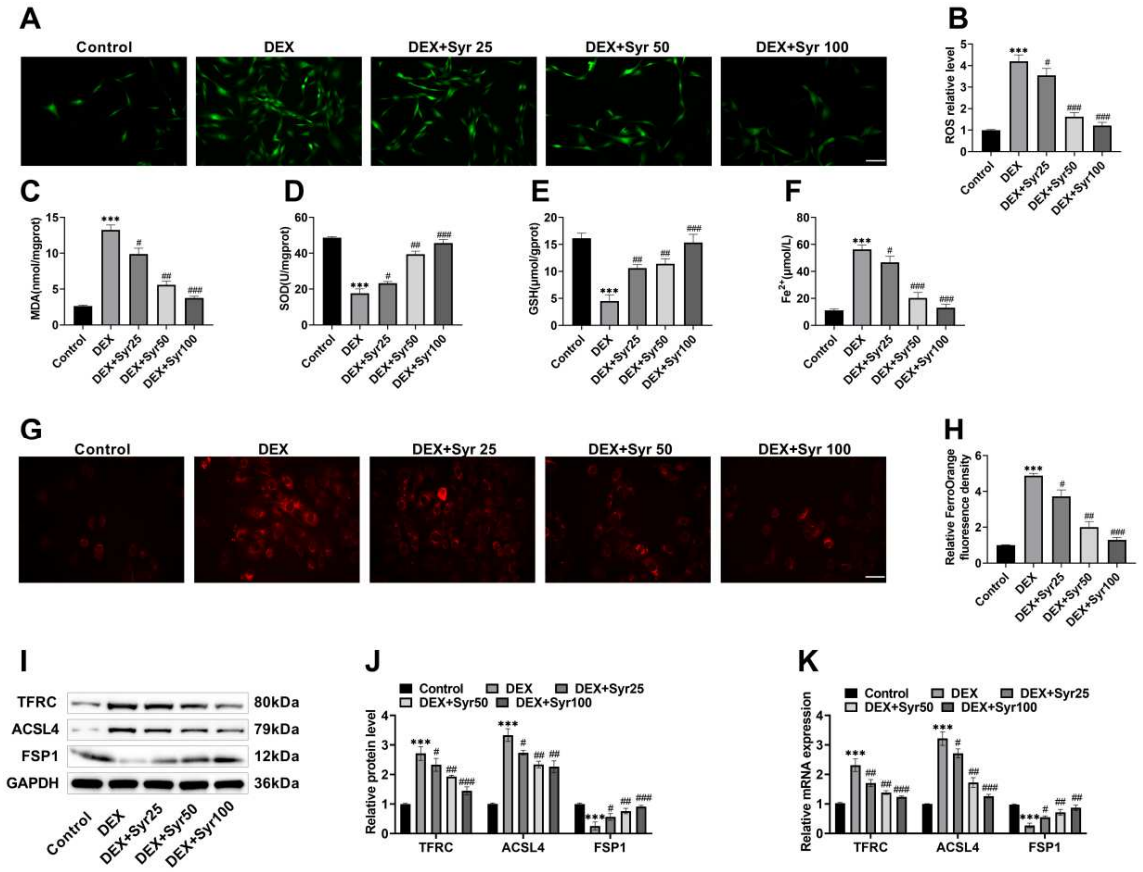

Fig. 3: Syr ameliorates DEX-induced oxidative stress and ferroptosis (A-B) Flow cytometry assessed ROS levels in MC3T3-E1 cells (40×, 50 μm). (C-E) Different kits assessed MDA, SOD, and GSH levels. (F) The results of the kit assay indicated that DEX treatment resulted in increased Fe^{2+} levels, while Syr treatment decreased Fe^{2+} levels. (G-H) FerroOrange fluorescent staining showed that DEX treatment increased Fe^{2+} content in MC3T3-E1 cells, while Syr treatment decreased Fe^{2+} content (40×, 50 μm). (I-J) Western blot measured TFRC, ACSL4 and FSP1 levels in MC3T3-E1 cells. (K) RT-qPCR measured that DEX up-regulated TFRC and ACSL4 and down-regulated FSP1, whereas Syr treatment reduced the effects of DEX. n=3, ***P<0.001 vs Control, #P<0.05, ##P<0.01, ###P<0.001 vs DEX.

injury model. DEX treatment reduced MC3T3-E1 cell activity and osteogenic ability, confirming the success of OP cell injury model construction. Of interest, Syr, as a natural lignan-like compound, is abundantly present in a variety of herbal medicines and plants and has been shown to alleviate osteoarthritis (Wang *et al.*, 2023c).

In this study, Syr at concentrations of 25, 50 and 100 μM had no adverse impact on normal MC3T3-E1 cell viability, yet effectively increased the viability of DEX-treated cells, inhibited LDH release and could promote the osteogenic differentiation of the cells. This confirms that Syr can promote osteogenesis and alleviate the progression of OP, offering a crucial experimental foundation for creating therapeutic drugs for OP with both high efficiency and safety. Decreased bone formation is one of the core pathological features of OP, which is strongly related to defects in differentiation and function of osteoblasts (Zhivodernikov *et al.*, 2023). During bone formation, preosteoblasts first proliferate, subsequently transform into mature osteoblasts and finally form a new bone matrix (Kitaura *et al.*, 2020). Runx2 is a key transcription factor that initiates osteoblast-specific gene expression and promotes differentiation of precursor cells to osteoblasts (Komori, 2022; Arya *et al.*, 2024). In cases where the Runx2 gene is defective, the development of osteoblasts and the process of bone formation in mice are severely impaired, leading to a diminished response to vitamin D (Aoki *et al.*, 2022). Bmp2 is a key cytokine that induces osteogenic differentiation and bone formation, promotes bone matrix synthesis and mineralized nodule formation and enhances osteoblast function (Chen *et al.*, 2022). After entering the late differentiation stage, the non-collagenous proteins OPN and OCN in the bone matrix play a key role. OPN mediates the adhesion of osteoblasts to the extracellular matrix, promotes bone mineralization and regulates bone remodeling homeostasis (Bai *et al.*, 2022). OCN, on the other hand, is directly involved in bone matrix mineralization as a hallmark protein of terminal osteoblast differentiation and its expression represents a late stage of osteoblast differentiation and maturation (Komori, 2020). In this study, Syr was able to promote the synthesis and secretion of the above osteogenesis-related proteins and also upregulated their expression.

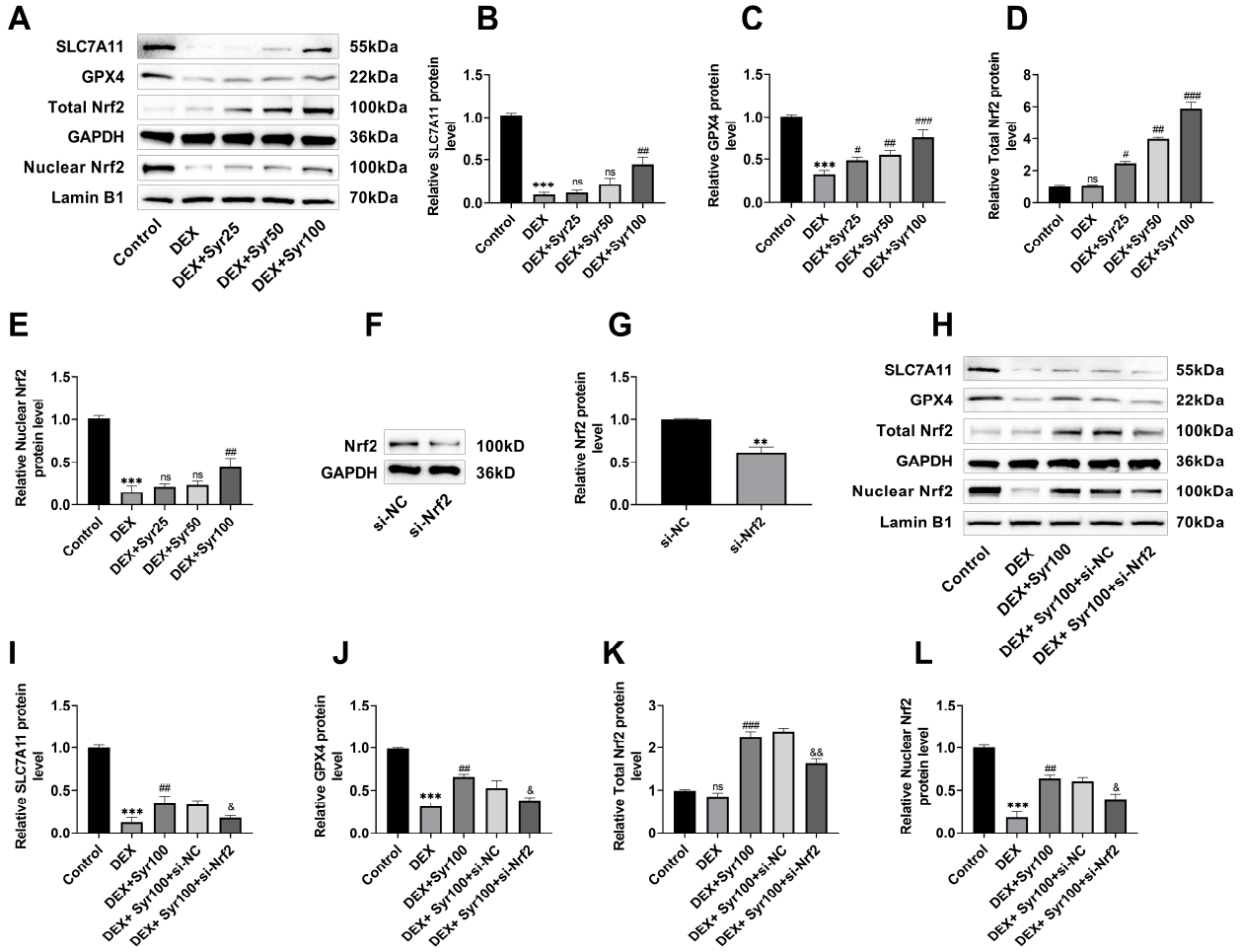

Fig. 4: Syr modulates Nrf2/SLC7A11/GPX4 signaling pathway (A-E) Western blot measured nuclear Nrf2, SLC7A11, GPX4, and Total Nrf2 in MC3T3-E1 cells. (F-G) Western blot indicated that transfection of si-Nrf2 resulted in declined Nrf2 level. (H-L) Western blot indicated that transfection of si-Nrf2 resulted in declined Nrf2, SLC7A11, Total Nrf2, nuclear Nrf2 and GPX4 protein levels. n=3, ns $P \geq 0.05$, ** $P<0.01$, *** $P<0.001$ vs Control; ns $P \geq 0.05$, # $P<0.05$, ## $P<0.01$, ### $P<0.001$ vs DEX, & $P<0.05$, && $P<0.01$ vs DEX+Syr+si-NC.

Therefore, we hypothesized that Syr could synergistically regulate bone formation by the cascade pathway of "transcriptional regulation (Runx2/Bmp2)-matrix synthesis (OPN)-mineralization and maturation (OCN)". In addition, cell staining results also showed that Syr increased ALP activity and promoted cell mineralization nodule formation. The study of Imtiyaz *et al*. also confirmed that Syr isolated from *Euonymus spraguei Hayata* increased ALP activity and mineral deposition in osteoblasts, which could promote osteogenic differentiation and have potential anti-OP effects (Imtiyaz *et al.*, 2020).

In recent years, the link between abnormal iron metabolism and a variety of metabolic bone diseases has received increasing attention and there is growing evidence that iron accumulation has adverse effects on bone health (Che *et al.*, 2020; Zhen *et al.*, 2025). Ferroptosis has been identified as a key factor in iron-overload-mediated bone homeostasis imbalance through activation of oxidative stress pathways (Gao *et al.*, 2022). Previous studies have pointed out that iron accumulation may disrupt bone homeostasis through two main mechanisms: by inhibiting osteoblast activity and promoting osteoclast differentiation, which leads to accelerated bone loss and consequently OP and ultimately an increased risk of fracture (Li *et al.*, 2023b). Recent studies have shown that blocking ferroptosis triggered by glucocorticoids in human bone marrow mesenchymal stem cells enhances cell proliferation and osteogenic differentiation (Zhao *et al.*, 2025). This suggests that targeted inhibition of ferroptosis might be an effective strategy for OP treatment. In this study, DEX treatment resulted in oxidative stress and raised Fe^{2+} levels and ferroptosis-related protein levels and declined ferroptosis-inhibiting protein levels. Syr treatment, on the other hand, effectively reversed the effect of DEX, which not only reduced ROS, MDA and Fe^{2+} levels, restored the antioxidant capacity of SOD and GSH, but also regulated ferroptosis-related protein expression.

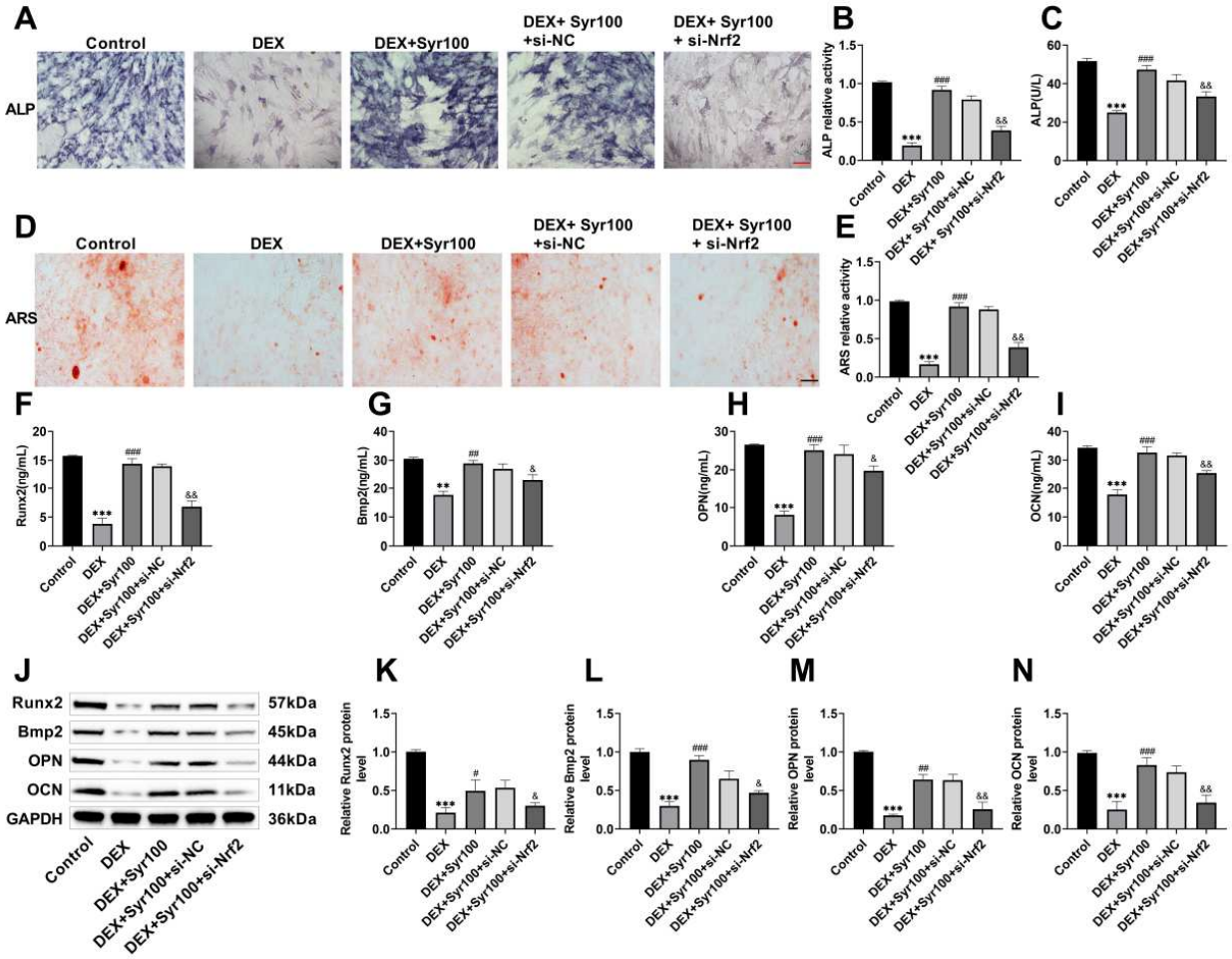

Fig. 5: Syr mediates the Nrf2/SLC7A11/GPX4 pathway to improve osteogenesis (A-C) ALP staining revealed measured Syr treatment elevated the differentiation activity, and transfection with si-Nrf2 attenuated the effect of Syr (20×, 100 μm). (D-E) ARS staining demonstrated that Syr increased the mineralization capacity, and transfection with si-Nrf2 decreased the mineralization capacity (20×, 100 μm). (F-I) ELISA kit measured Runx2, OPN and OCN levels in the cell supernatant. (J-N) Western blot measured Runx2, OPN, and OCN proteins levels in MC3T3-E1 cells. n=3, ***P*<0.01, ****P*<0.001 vs Control; #*P*<0.05, ##*P*<0.01, ###*P*<0.001 vs DEX, &*P*<0.05, &&*P*<0.01 vs DEX+Svr+si-NC.

This suggests that Syr is protective against DEX-triggered ferroptosis in osteoblasts through a multi-targeted regulation of iron metabolism and oxidative stress network. Iron chelating inhibitor desferrioxamine (DFO) inhibits ferroptosis by directly chelating intracellular free iron (Fe^{2+}), reduces iron-dependent lipid peroxidation and attenuates osteoclast ferroptosis and ameliorates bone loss in the OP model (Che *et al.*, 2020; Ma *et al.*, 2020; Jiang *et al.*, 2022). Compared with DFO, Syr does not rely on the direct chelation of iron ions, but activates the Nrf2/SLC7A11/GPX4 signaling pathway to up-regulate the expression of FSP1, down-regulate the expression of TFRC and ACSL4, reduce the level of cytoplasmic free iron and at the same time, reduce the level of ROS, MDA and both the "iron metabolism regulation" and "anti-oxidative stress" dual role. Nrf2 serves as a core regulator of the cellular oxidative stress response, is important in regulating lipid peroxidation reduction and hindering free iron accumulation (Han *et al.*, 2024). Nrf2 is regarded as a core inhibitor of ferroptosis and abnormal Nrf2 signaling (e.g., Nrf2 inactivation or impaired nuclear translocation) can lead to down-regulation of proteins like SLC7A11 and GPX4, which disrupts redox homeostasis and ultimately induces ferroptosis (Ding *et al.*, 2023; Li *et al.*, 2024). Zhang *et al*. showed that activation of Nrf2 signaling elevated SLC7A11 and GPX4 levels, which could inhibit ferroptosis in osteoblasts (Zhang *et al.*, 2022b). Deng *et al*. found that Mangiferin activated Nrf2/SLC7A11/GPX4 pathway and promoted bone formation in OP model mice, but did not alleviate OP symptoms in Nrf2 knockout mice (Deng *et al.*, 2024). These investigations reveal that the Nrf2/SLC7A11/GPX4 pathway is crucial in ferroptosis and OP progression. Based on this, the present study further investigated whether Syr inhibits DEX-mediated ferroptosis through regulating the Nrf2/SLC7A11/GPX4 pathway in MC3T3-E1 cells, which in turn inhibits OP progression.

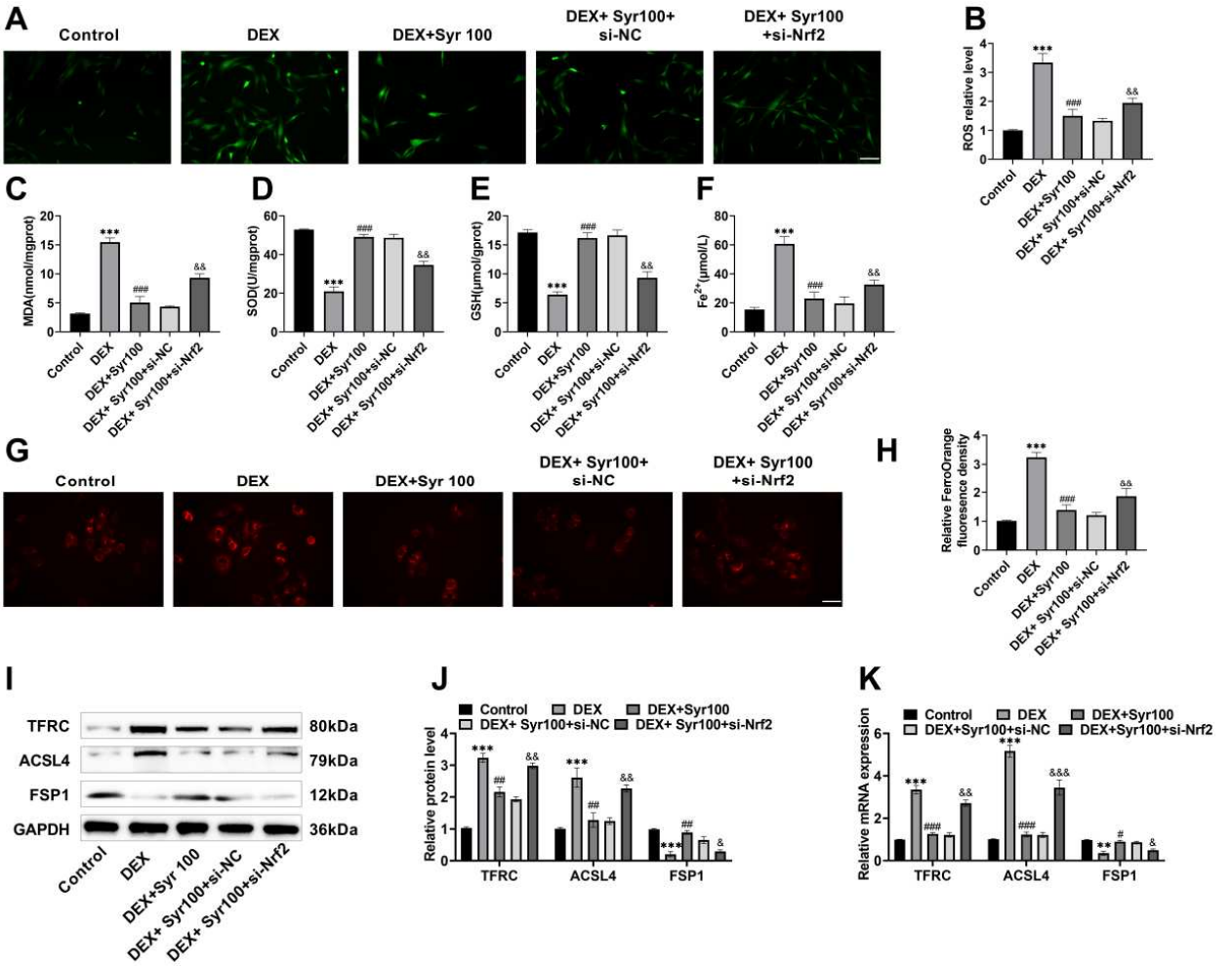

Fig. 6: Syr mediates the Nrf2/SLC7A11/GPX4 signaling pathway to ameliorate oxidative stress and ferroptosis caused by DEX (A-B) Flow cytometry assessed ROS levels in MC3T3-E1 cells transfection with si-Nrf2 (40×, 50 μm). (C-E) Different kits assessed MDA, SOD, and GSH levels in MC3T3-E1 cells transfection with si-Nrf2. (F) The kit assay indicated that Syr caused a decline in Fe^{2+} level and silencing Nrf2 increased Fe^{2+} levels. (G-H) FerroOrange fluorescent staining showed that Syr treatment decreased Fe^{2+} content in MC3T3-E1 cells, whereas silencing Nrf2 increased Fe^{2+} content (40×, 50 μm). (I-J) Western blot measured TFRC, ACSL4, and FSP1 levels. (K) RT-qPCR measured that Syr down-regulated TFRC and ACSL4 and up-regulated FSP1, whereas silencing Nrf2 reduced the effects of Syr. n=3, ***P<0.001 vs Control; ##P<0.01, ###P<0.001 vs DEX, &&P<0.01vs DEX+Syr+si-NC.

We found that SLC7A11, GPX4 and nuclear Nrf2 levels were reduced in MC3T3-E1 cells after DEX treatment, whereas the Total Nrf2 protein level did not change significantly, suggesting that DEX may inhibit pathway activation by blocking Nrf2 translocation to the nucleus. In contrast, Syr treatment increased SLC7A11, GPX4, nuclear Nrf2 and total Nrf2 levels, suggesting that Syr promotes Nrf2 nuclear translocation and activates the Nrf2/SLC7A11/GPX4 pathway. After transfection of si-Nrf2, the ameliorative impacts of Syr on osteogenic function and ferroptosis were significantly attenuated, with a marked decrease in cellular osteogenic differentiation-related indexes and a rebound in the levels of ferroptosis markers. This suggests that the ameliorative effect of Syr on DEX-induced osteoblast injury and ferroptosis is highly dependent on the activation of the Nrf2/SLC7A11/GPX4 pathway.

The role of Syr in the regulation of ferroptosis and its impact on osteogenic differentiation has been the main focus of our study. However, other osteogenic signaling pathways may also play important roles in this process and the roles of other pathways can be further explored in the future. In addition, Syr may also affect cell function through other non-ferroptosis-related pathways. Specific inhibitors or knockdown techniques could be used in subsequent studies to verify whether the effects of Syr are realized through the ferroptosis pathway. Cells may activate compensatory pathways to maintain cellular function under stress conditions and changes in other cellular stress markers may be examined in subsequent studies to determine whether there is activation of compensatory pathways. In subsequent research, the effect of Syr in other osteocyte lines can be tested to further evaluate whether the role of Syr is cell type-specific or

whether it can be extended to other osteocytes. Furthermore, long-term safety assessment and bioavailability studies of Syr are needed in the future. All experiments were conducted in vitro; therefore, the efficacy of Syr *in-vivo* remains to be validated.

CONCLUSION

Syr can alleviate DEX-induced MC3T3-E1 cell injury and ferroptosis by stimulating the Nrf2/SLC7A11/GPX4 pathway, improve osteogenic function and have potential for the treatment of OP. This research reveals the function of Syr in bone metabolism, clarifies it as a potential OP therapeutic agent and provides a basis for the development of OP therapeutics based on Nrf2 pathway activation. However, this study still has some limitations, focusing only on a single pathway and OP pathogenesis involves multifactorial factors; future studies should focus on examining the relationship between this pathway and other bone metabolism pathways, as well as determining the treatment efficacy via *in-vivo* experiments. While these findings are promising, *in-vivo* studies are required to confirm Syr's efficacy and safety for clinical use in OP.

Acknowledgment
Not applicable.

Authors' contributions
[Shaojing Wang]: Conducted and designed the research, carried out experiments and analyzed findings. Edited and refined the manuscript with a focus on critical intellectual contributions.
[Guoying Zhang]: Participated in collecting, assessing and interpreting the data. Made significant contributions to data interpretation and manuscript preparation.
[Shaojing Wang, Guoying Zhang]: Provided substantial intellectual input during the drafting and revision of the manuscript.

The final version of the manuscript has been reviewed and approved by all authors.

Funding
There was no funding.

Data availability statement
The data supporting the findings of this study can be obtained from the corresponding author, Guoying Zhang, upon request.

Ethical approval
Not applicable.

Conflicts of interest
The authors affirm that they do not have any conflicts of interest.

REFERENCES

Aoki H, Suzuki E, Nakamura T, Onodera S, Saito A, Ohtaka M, Nakanishi M, Nishimura K, Saito A and Azuma T (2022). Induced pluripotent stem cells from homozygous Runx2-deficient mice show poor response to vitamin D during osteoblastic differentiation. *Med Mol Morphol*., **55**(3): 174-186.

Arya PN, Saranya I and Selvamurugan N (2024). RUNX2 regulation in osteoblast differentiation: A possible therapeutic function of the lncRNA and miRNA-mediated network. *Differentiation*. **140**: 100803.

Ashrafizadeh M (2024). Cell death mechanisms in human cancers: Molecular pathways, therapy resistance and therapeutic perspective. *JCBT.,* **1**(1): 17-40.

Bai R J, Li Y S and Zhang F J (2022). Osteopontin, a bridge links osteoarthritis and osteoporosis. *Front Endocrinol (Lausanne)*. **13**: 1012508.

Brown JP (2021). Long-term treatment of postmenopausal osteoporosis. *Endocrinol Metab (Seoul)*. **36**(3): 544-552.

Che J, Yang J, Zhao B, Zhang G, Wang L, Peng S and Shang P (2020). The effect of abnormal iron metabolism on osteoporosis. *Biol Trace Elem Res*. **195**(2): 353-365.

Chen L, Liu H, Sun C, Pei J, Li J, Li Y, Wei K, Wang X, Wang P, Li F, Gai S, Zhao Y and Zheng Z (2022). A novel LncRNA SNHG3 promotes osteoblast differentiation through BMP2 upregulation in aortic valve calcification. *JACC Basic Transl Sci*. **7**(9): 899-914.

Clynes M A, Harvey N C, Curtis E M, Fuggle N R, Dennison E M and Cooper C (2020). The epidemiology of osteoporosis. *Br Med Bull*. **133**(1): 105-117.

Deng X, Lin B, Wang F, Xu P and Wang N (2024). Mangiferin attenuates osteoporosis by inhibiting osteoblastic ferroptosis through Keap1/Nrf2/SLC7A11/GPX4 pathway. *Phytomedicine*. **124**: 155282.

Ding S, Duanmu X, Xu L, Zhu L and Wu Z (2023). Ozone pretreatment alleviates ischemiareperfusion injury-induced myocardial ferroptosis by activating the Nrf2/Slc7a11/Gpx4 axis. *Biomed Pharmacother*. **165**:115185.

Dixon S J and Olzmann J A (2024). The cell biology of ferroptosis. *Nat Rev Mol Cell Biol*. **25**(6): 424-442.

Fischer V and Haffner-Luntzer M (2022). Interaction between bone and immune cells: Implications for postmenopausal osteoporosis. *Semin Cell Dev Biol*. **123**: 14-21.

Gao Z, Chen Z, Xiong Z and Liu X (2022). Ferroptosis - A new target of osteoporosis. *Exp Gerontol*. **165**: 111836.

Han D, Gu X, Gao J, Wang Z, Liu G, Barkema H W and Han B (2019). Chlorogenic acid promotes the Nrf2/HO-1 anti-oxidative pathway by activating p21(Waf1/Cip1) to resist dexamethasone-induced apoptosis in osteoblastic cells. *Free Radic Biol Med*. **137**: 1-12.

Han H, Zhang G, Zhang X and Zhao Q (2024). Nrf2-mediated ferroptosis inhibition: a novel approach for

managing inflammatory diseases. *Inflammopharmacology*. **32**(5): 2961-2986.

Imtiyaz Z, Lin Y T, Cheong U H, Jassey A, Liu H K and Lee M H (2020). Compounds isolated from Euonymus spraguei Hayata induce ossification through multiple pathways. *Saudi J Biol Sci*. **27**(9): 2227-2237.

Jang W Y, Kim M Y and Cho J Y (2022). Antioxidant, anti-inflammatory, anti-menopausal, and anti-cancer effects of lignans and their metabolites. *Int J Mol Sci*. **23**(24): 15482.

Jha SS (2023). Glucocorticoid-induced osteoporosis (GIOP). *Indian J Orthop*. **57**(Suppl 1): 181-191.

Jiang X, Stockwell B R and Conrad M (2021). Ferroptosis: mechanisms, biology and role in disease. *Nat Rev Mol Cell Biol*. **22**(4): 266-282.

Jiang Z, Wang H, Qi G, Jiang C, Chen K and Yan Z (2022). Iron overload-induced ferroptosis of osteoblasts inhibits osteogenesis and promotes osteoporosis: An in vitro and in vivo study. *IUBMB Life*. **74**(11): 1052-1069.

Johnston C B and Dagar M (2020). Osteoporosis in Older Adults. *Med Clin North Am*. **104**(5): 873-884.

Kim J M, Lin C, Stavre Z, Greenblatt M B and Shim J H (2020). Osteoblast-Osteoclast Communication and Bone Homeostasis. *Cells*. **9**(9): 2073.

Kirsch V, Bakuradze T and Richling E (2020). Toxicological testing of syringaresinol and enterolignans. *Curr Res Toxicol*. **1**: 104-110.

Kitaura H, Marahleh A, Ohori F, Noguchi T, Shen W R, Qi J, Nara Y, Pramusita A, Kinjo R and Mizoguchi I (2020). Osteocyte-related cytokines regulate osteoclast formation and bone resorption. *Int J Mol Sci*. **21**(14): 5169.

Komori T (2020). Functions of osteocalcin in bone, pancreas, testis, and muscle. *Int J Mol Sci*. **21**(20): 7513.

Komori T (2022). Whole aspect of Runx2 functions in skeletal development. *Int J Mol Sci*. **23**(10): 5776.

Li G F, Gao Y, Weinberg E D, Huang X and Xu Y J (2023b). Role of Iron Accumulation in Osteoporosis and the underlying mechanisms. *Curr Med Sci*. **43**(4): 647-654.

Li G, Liu C, Yang L, Feng L, Zhang S, An J, Li J, Gao Y, Pan Z, Xu Y, Liu J, Wang Y, Yan J, Cui J, Qi Z and Yang L (2023a). Syringaresinol protects against diabetic nephropathy by inhibiting pyroptosis via NRF2-mediated antioxidant pathway. *Cell Biol Toxicol*. **39**(3): 621-639.

Li S, Zhang Y, Ding S, Chang J, Liu G and Hu S (2025). Curcumin ameliorated glucocorticoid-induced osteoporosis while modulating the gut microbiota and serum metabolome. *J Agric Food Chem*. **73**(14): 8254-8276.

Li W, Wang Y, Zhang Y, Fan Y, Liu J, Zhu K, Jiang S and Duan J (2024). Lizhong decoction ameliorates ulcerative colitis by inhibiting ferroptosis of enterocytes via the Nrf2/SLC7A11/GPX4 pathway. *J Ethnopharmacol*. **326**: 117966.

Liu H, Zhang T A, Zhang W Y, Huang S R, Hu Y and Sun J (2023). Rhein attenuates cerebral ischemia-reperfusion injury via inhibition of ferroptosis through NRF2/SLC7A11/GPX4 pathway. *Exp Neurol*. **369**:114541.

Liu P, Wang W, Li Z, Li Y, Yu X, Tu J and Zhang Z (2022). Ferroptosis: A new regulatory mechanism in osteoporosis. *Oxid Med Cell Longev*. **2022**: 2634431.

Lo JC, Yang W, Park-Sigal JJ and Ott SM (2023). Osteoporosis and Fracture Risk among Older US Asian Adults. *Curr Osteoporos Rep*. **21**(5): 592-608.

Ma H, Wang X, Zhang W, Li H, Zhao W, Sun J and Yang M (2020). Melatonin suppresses ferroptosis induced by high glucose via activation of the Nrf2/HO-1 signaling pathway in type 2 diabetic osteoporosis. *Oxid Med Cell Longev*. **2020**: 9067610.

Madrid A, Lamm C and Aeberli D (2025). Glucocorticoid-induced osteoporosis; epidemiology, pathogenesis and treatment. *Ther Umsch*. **82**(1): 20-25.

Morgenstern C, Lastres-Becker I, Demirdöğen B C, Costa V M, Daiber A, Foresti R, Motterlini R, Kalyoncu S, Arioz B I, Genc S, Jakubowska M, Trougakos I P, Piechota-Polanczyk A, Mickael M, Santos M, Kensler T W, Cuadrado A and Copple I M (2024). Biomarkers of NRF2 signalling: Current status and future challenges. *Redox Biol*. **72**: 103134.

Muñoz M, Robinson K and Shibli-Rahhal A (2020). Bone health and osteoporosis prevention and treatment. *Clin Obstet Gynecol*. **63**(4): 770-787.

Ochiai N, Etani Y, Noguchi T, Miura T, Kurihara T, Fukuda Y, Hamada H, Uemura K, Takashima K, Tamaki M, Ishibashi T, Ito S, Yamakawa S, Kanamoto T, Okada S, Nakata K and Ebina K (2024). The pivotal role of the Hes1/Piezo1 pathway in the pathophysiology of glucocorticoid-induced osteoporosis. *JCI Insight*. **9**(23): e179963.

Pandarathodiyil A K, Ramanathan A, Garg R, Doss J G, Rahman F B A, Ghani W M N and Vijayan S P (2022). Lactate Dehydrogenase: The Beacon of Hope? *J Pharm Bioallied Sci*. **14**(Suppl 1): S1090-s1092.

Qiao H, Ren H, Liu Q, Jiang Y, Wang Q, Zhang H, Gan L, Wang P, Cui Y, Wang J, Chou Y, Chen L, Shi J and Dou Y (2025). Anti-inflammatory effects of *Rehmannia glutinosa* polysaccharide on LPS-induced acute liver injury in mice and related underlying mechanisms. *J Ethnopharmacol*. **351**:120099.

Sabri S A, Chavarria J C, Ackert-Bicknell C, Swanson C and Burger E (2023). Osteoporosis: An update on screening, diagnosis, evaluation, and treatment. *Orthopedics*. **46**(1): e20-e26.

Urquiaga M and Saag K G (2022). Risk for osteoporosis and fracture with glucocorticoids. *Best Pract Res Clin Rheumatol*. **36**(3): 101793.

Walker MD and Shane E (2023). Postmenopausal Osteoporosis. *N Engl J Med*. **389**(21): 1979-1991.

Wang D, Shen J, Wang Y, Cui H, Li Y, Zhou L, Li G, Wang Q, Feng X, Qin M, Dong B, Yang P, Li Y, Ma X and Ma J (2025). Mechanisms of ferroptosis in bone disease: A

new target for osteoporosis treatment. *Cell Signal*. **127**: 111598.

Wang H, Yu X, Liu D, Qiao Y, Huo J, Pan S, Zhou L, Wang R, Feng Q and Liu Z (2024a). VDR activation attenuates renal tubular epithelial cell ferroptosis by regulating Nrf2/HO-1 signaling pathway in diabetic nephropathy. *Adv Sci (Weinh)*. **11**(10): e2305563.

Wang J, Chen T and Gao F (2024b). Mechanism and application prospect of ferroptosis inhibitors in improving osteoporosis. *Front Endocrinol (Lausanne)*. **15**:1492610.

Wang J, Shu B, Tang D Z, Li C G, Xie X W, Jiang L J, Jiang X B, Chen B L, Lin X C, Wei X, Leng X Y, Liao Z Y, Li B L, Zhang Y, Cui X J, Zhang Q, Lu S, Shi Q and Wang Y J (2023a). The prevalence of osteoporosis in China, a community based cohort study of osteoporosis. *Front Public Health*. **11**: 1084005.

Wang J, Zou J, Zhao C, Yu H, Teng J and Dong L (2023b). Syringaresinol inhibits cardiorenal fibrosis through HSP90 in a cardiorenal syndrome type 2. *Hum Exp Toxicol*. **42**: 9603271231165678.

Wang X, Wang D, Deng B and Yan L (2023c). Syringaresinol attenuates osteoarthritis via regulating the NF-κB pathway. *Int Immunopharmacol*. **118**: 109982.

Wang Y, Wang X, Wang K, Qin W and Li N (2024c). Extract of *Curculigo capitulata* ameliorates postmenopausal osteoporosis by promoting osteoblast proliferation and differentiation. *Cells*. **13**(23): 2028.

Wang Z, Jones G, Winzenberg T, Cai G, Laslett L L, Aitken D, Hopper I, Singh A, Jones R, Fripp J, Ding C and Antony B (2020). Effectiveness of *curcuma longa* extract for the treatment of symptoms and effusion-synovitis of knee osteoarthritis: A Randomized Trial. *Ann Intern Med*. **173**(11): 861-869.

Wu X, Fang X, Lu F, Chen Q, Liu J and Zheng L (2024a). An update on the role of ferroptosis in the pathogenesis of osteoporosis. *EFORT Open Rev*., **9**(8): 712-722.

Wu Z, Li W, Jiang K, Lin Z, Qian C, Wu M, Xia Y, Li N, Zhang H, Xiao H, Bai J and Geng D (2024b). Regulation of bone homeostasis: Signaling pathways and therapeutic targets. *MedComm (2020)*. **5**(8): e657.

Yao X W, Liu Z Y, Ma N F, Jiang W K, Zhou Z, Chen B, Guan W G, Yan J J and Yang M (2023). Exosomes from adipose-derived stem cells alleviate dexamethasone-induced bone loss by regulating the Nrf2/HO-1 Axis. *Oxid Med Cell Longev*., **2023**:3602962.

Yong E L and Logan S (2021). Menopausal osteoporosis: screening, prevention and treatment. *Singapore Med J*. **62**(4): 159-166.

Yuan Y, Zhai Y, Chen J, Xu X and Wang H (2021). Kaempferol ameliorates oxygen-glucose deprivation/reoxygenation-induced neuronal ferroptosis by activating Nrf2/SLC7A11/GPX4 Axis. *Biomolecules*. **11**(7): 923.

Zhang L, Tian Y, Zhang L, Zhang H, Yang J, Wang Y, Lu N, Guo W and Wang L (2025). A comprehensive review on the plant sources, pharmacological activities and pharmacokinetic characteristics of Syringaresinol. *Pharmacol Res*., **212**: 107572.

Zhang M, Chen D, Zeng N, Liu Z, Chen X, Xiao H, Xiao L, Liu Z, Dong Y and Zheng J (2022a). Hesperidin ameliorates dexamethasone-induced osteoporosis by inhibiting p53. *Front Cell Dev Biol*. **10**: 820922.

Zhang X, Xu X, Zhang C, Xu C, Huang F and Xie W (2024). Comparison of the effectiveness of teriparatide and zoledronic acid in osteoporosis treatment: A meta-analysis. **20**(4): 690-697.

Zhang Z, Ji C, Wang Y N, Liu S, Wang M, Xu X and Zhang D (2022b). Maresin1 Suppresses High-Glucose-Induced Ferroptosis in Osteoblasts via NRF2 Activation in Type 2 Diabetic Osteoporosis. *Cells*. **11**(16): 2560.

Zhao R, Tao L, Qiu S, Shen L, Tian Y, Gong Z, Tao Z B and Zhu Y (2020). Melatonin rescues glucocorticoid-induced inhibition of osteoblast differentiation in MC3T3-E1 cells via the PI3K/AKT and BMP/Smad signalling pathways. *Life Sci*. **257**: 118044.

Zhao Z M, Ding J M, Li Y, Wang D C and Kuang M J (2025). Human umbilical cord mesenchymal stem cell-derived exosomes promote osteogenesis in glucocorticoid-induced osteoporosis through PI3K/AKT signaling pathway-mediated ferroptosis inhibition. *Stem Cells Transl Med*. **14**(3): szae096.

Zhen C, Wang S, Yang J, Zhang G, Cai C, Wang J, Wang A, Xu Y, Fang Y, Wei M, Yin D, Luo X, Gong M, Zhang H and Shang P (2025). Moderate static magnetic field regulates iron metabolism and salvage bone loss caused by iron accumulation. *J Orthop Translat*. **50**: 144-157.

Zheng Y, Sun R, Yang H, Gu T, Han M, Yu C, Chen P, Zhang J, Jiang T, Ding Y, Liang L, Quan R, Yao S and Zhao X (2025). Aucubin promotes BMSCs proliferation and differentiation of postmenopausal osteoporosis patients by regulating ferroptosis and bmp2 signalling. *J Cell Mol Med*. **29**(2): e70288.

Zheng Y, Xiao Y, Zhang D, Zhang S, Ouyang J, Li L, Shi W, Zhang R, Liu H, Jin Q, Chen Z, Xu D and Wu L (2021). Geniposide ameliorated dexamethasone-induced cholesterol accumulation in osteoblasts by mediating the GLP-1R/ABCA1 Axis. *Cells*. **10**(12): 3424.

Zhivodernikov IV, Kirichenko TV, Markina YV, Postnov AY and Markin AM (2023). Molecular and cellular mechanisms of osteoporosis. *Int J Mol Sci*. **24**(21): 15772.

Zhong D, Li X, Yin Z, Chen P, Li Y, Tian J, Wang L, Liu H, Yin K, Zhu L, Kong L, Chen K, Li Y, Hong C and Wang C (2025). Circ-ITCH promotes the ubiquitination degradation of HOXC10 to facilitate osteogenic differentiation in disuse osteoporosis through stabilizing BRCA1 mRNA via IGF2BP2-mediated m(6)A modification. *J Transl Med*. **23**(1): 376.

Zhu J, Feng C, Zhang W, Wang Z, Zhong M, Tang W, Wang Z, Shi H, Yin Z, Shi J, Huang Y, Xiao L, Geng D and Wang Z (2022). Activation of dopamine receptor D1

promotes osteogenic differentiation and reduces glucocorticoid-induced bone loss by upregulating the ERK1/2 signaling pathway. *Mol Med*. **28**(1): 23.

Zou Y C, Gao K, Cao B T, He X L, Zheng W, Wang X F, Li Y F, Li F and Wang H J (2024). Syringin protects high glucose-induced BMSC injury, cell senescence, and osteoporosis by inhibiting JAK2/STAT3 signaling. *J Appl Biomed*. **22**(4): 197-207.